World J Microbiol Biotechnol (2015) 31:1343–1352
DOI 10.1007/s11274-015-1877-3

ORIGINAL PAPER

Involvement of an alternative oxidase in the regulation of hyphal growth and microsclerotial formation in *Nomuraea rileyi* CQNr01

Guilin Zhou[1] · Zhangyong Song[1] · Youping Yin[1] · Wei Jiang[1] · Zhongkang Wang[1]

Received: 14 January 2015 / Accepted: 20 May 2015 / Published online: 2 July 2015

Abstract Mitochondria of *Nomuraea rileyi* contain an alternative oxidase (Aox), which reduces oxygen to water by accepting electrons directly from ubiquinol. Furthermore, through a transcriptional analysis, we found that an alternative oxidase (*Nraox*) was up-regulated during microsclerotial formation. To study the function of NrAox, *Nraox* was cloned from *N. rileyi* CQNr01. The full-length cDNA was 1266 bp with an open reading frame of 1068 bp encoding 355 amino acids. A phylogenetic analysis revealed that the NrAox of *N. rileyi* was closely related to *Metarhizium acridum* Aox. The relative expression level of the *Nraox* was up-regulated during microsclerotial (MS) initiation. A salicylhydroxamic acid, a specific alternative oxidase inhibitor, application to the culture media severely decreased MS yields, changed the hyphae morphology and slowed the H_2O_2 removal. *Nraox* silencing caused mycelial deformations, reduced the MS yields by 97.3 % and increased MS size compared with those of the control. MS virulence was decreased to 26.2 % after *Nraox* was silenced. However, the *Nraox*-silenced strain was sensitive to environmental stress, and the growth rate was reduced under stress conditions. The results obtained suggested that *Nraox* is required for MS differentiation by regulating the intracellular H_2O_2 concentration and hypha growth. Additionally, *Nraox* had a great impact on the virulence of *N. rileyi*.

Keywords Microsclerotia · Alternative oxidase · *Nomuraea rileyi* · Oxidative stress · RNA interference

Introduction

The clavicipitaceae *Nomuraea rileyi* is a cosmopolitan, filamentous, dimorphic entomogenous fungus. It infects many noctuid pests, causing insect disease in natural environments (Suwannakut et al. 2005), hence it has the potential to be developed into a mycoinsecticide (Thakre et al. 2011). However, its sporulation requires fastidious growth conditions, such as a specific carbon source (maltose) and light stimulation, which limit its mass production and commercialization (Faria and Wraight 2007). Therefore, it is necessary to find an easy-to-scale production method with effective ingredients.

The microsclerotia (MS) of *N. rileyi* is a diameter of 50–600 μm pseudoparenchyma formed by pigmented, compact aggregation of mycelia that is highly resistant to desiccation and its formation has been successfully induced by liquid amended medium (AM) in our laboratory (Yin et al. 2012). The resistance and stability of microsclerotia allow them to act as propagules since they can withstand adverse environmental conditions. Additionally, they exhibit a highly insecticidal activity against *Spodoptera litura*, and thus, can be used as an alternative active instead of conidia in pest biocontrol (Yin et al. 2012; Song et al. 2014).

Previous studies on the mechanisms of sclerotial differentiation mainly focused on plant pathogenic fungi.

Electronic supplementary material The online version of this article (doi:10.1007/s11274-015-1877-3) contains supplementary material, which is available to authorized users.

✉ Zhongkang Wang
w-zk@163.com

[1] Chongqing Engineering Research Center for Fungal Insecticides, School of Life Science, Chongqing University, Chongqing 400030, China

Sclerotial differentiation may be associated with oxidative stress and accompanied by high lipid peroxidation (Georgiou 1997; Georgiou et al. 2006). Additionally, the hydroxyl radical scavengers can inhibit or delay the formation of sclerotia in other sclerotia-producing fungi (Georgiou et al. 2000a, b). Our preliminary experiments showed that the MS formation of *N. rileyi* is closely related to oxidative stress and that a large amount of reducing enzymes or synthetic reducing substances are up-regulated during MS differentiation (Jiang et al. 2014; Liu et al. 2014; Song et al. 2013). However, the role of detoxifying-reducing enzymes or reducing substances in detoxifying oxidative stress in MS development has not been reported.

Reactive oxygen species (ROS) including superoxide radicals, hydroxyl radicals and H_2O_2 are generated from the respiratory chain complex I and III (Harman 1956, 1981, 1998). In most fungi and higher plants, there are two respiratory electron transport chains in mitochondria: one is the classical respiratory chain with cyanide-sensitive cytochrome oxidase as the terminal oxidase, and the other is the alternative pathway, that branches from the inner mitochondrial membrane at the site of the ubiquinone pool and uses the alternative oxidase (Aox) as its terminal oxidase. The alternative pathway behaves as a short circuit to the main respiratory chain, which can be specifically inhibited by salicylhydroxamic acid (SHAM: Schonbaum et al. 1971; Vanlerberghe and Mclntosh 1997). The electron flux to Aox branches from the classical electron transport chain at the level of the ubiquinone pool leading to the direct reduction of oxygen to water, bypassing complex III and IV, which are two sites of energy conservation in the cell (Vanlerberghe and Mclntosh 1997). Therefore, Aox-mediated O_2 reduction is not coupled to proton pumping and oxidative phosphorylation. Most progress today in the field of Aox research has come from the kingdoms of plants, fungi and protists (McDonald 2008). Aox contributes to the reduction of ROS regulation of energy production and metabolism in fungi (Hattori et al. 2008; Helmerhorst et al. 2005; Ruy et al. 2006). Aox was proposed to play an important role in the oxidative stress defense mechanism (Joseph-Horne et al. 2001; Martins et al. 2011), but no studies have been performed relating to its functions in MS formation.

Our preliminary work demonstrated that the expression of the *Nraox* gene was up-regulated in microsclerotia development (Song et al. 2013). In this paper, the full length *Nraox* gene was cloned and the gene functions in MS development were studied using an expression pattern analysis and RNA interference (RNAi). The findings of this study provide new information on the contribution of *Nraox* in *N. rileyi* MS differentiation.

Materials and methods

Fungi strains and media

The *N. rileyi* CQNr01 strain was originally obtained from cadavers of *S. litura* infected naturally and stored at the Engineering Research Center for Fungal Insecticides, Chongqing University, China. The strain was grown on Sabouraud maltose agar fortified with 1 % yeast extract (SMAY) medium at 25 °C under the 12 dark/12 light intermittent illumination for 14 days. For the liquid culture, the conidia were suspended in sterile 0.05 % Tween 80 at 1×10^8 conidia/ml, and then inoculated into a 0.25-l Erlenmeyer flask containing 100 ml liquid AM media (Song et al. 2013) under continuous shock culturing (250 rpm) at 28 °C on rotary shakers.

Cloning the *Nraox* gene of CQNr01

Total RNA from CQNr01 was obtained using TRIzol® reagent (Invitrogen, USA). cDNA was synthesized from 2 μg of total RNA using SuperScript II reverse transcriptase according to the manufacturer's instructions (Invitrogen, USA). The full cDNAs sequences were obtained by the specific primer pairs designed based on the partial sequence data of *Nraox* from the comparative transcriptomic library (Song et al. 2013) using Primer Premier 5.0. The PCR product was cloned into pMD19-T vector (TaKaRa, Japan) and sequenced. The total genomic DNA of CQNr01 was extracted using the Biospin Fungus Genomic DNA Extraction kit (BioFlux, Japan). To acquire the genomic DNA sequence of *Nraox*, primers were designed and synthesized based on the full-length cDNA of *Nraox*. All of the primer sequences are shown in Supplementary Table S1. PCR was performed using total genomic DNA as the template. The sequencing of these PCR products was carried out in the same manner as described above.

Bioinformatics analysis of Nraox

The *Nraox* open reading frame (ORF) was identified using the NCBI ORF Finder (http://www.ncbi.nlm.nih.gov/gorf/gorf.html). The amino acid sequences were aligned by the DNAMAN program. To reconstruct the phylogenetic tree for *Nraox* genes, the protein sequences of the genes from different species were used as query sequences to search for homologous sequences of in the NCBI database (http://www.ncbi.nlm.nih.gov/). The phylogenetic tree was constructed by the neighbor-joining method with a bootstrap test calculated with 1000 replicates using MEGA version 4.1.

The expression pattern analysis of *Nraox* during MS development

To analyze the expression levels of the *Nraox* gene by Real-time quantitative PCR (RT-qPCR), total RNA was isolated, incubated with DNase I (Takara) and then tested using a conventional PCR with β-tubulin (*tub*) primers to confirm the absence of chromosomal DNA contamination (Goldman et al. 2003). DNAse-I-treated total RNA was used to synthesize the first strand cDNA using the Moloney marine leukemia virus reverse transcriptase (M-MLV RT) kit (Promega, Madison, WI, USA) following the manufacturer's instructions. RT-qPCR was performed using SYBR® Green II mix (Takara) according to the manufacturer's instructions. *Nraox* gene expression in MS development at different time points [germinating spore, yeast-like cells, MS initiation (SI) and MS formation] was evaluated. Two reference genes (house-keeping gene), translation elongation factor (*tef*) and *tub*, were used for normalizing the target gene's expression and correcting for sample-to-sample variation. The primers used in the experiments are shown in Supplementary Table S1. Relative gene expression levels were calculated using the $2^{-\Delta\Delta Ct}$ method (Livak and Schmittgen 2001). Each experiment was performed in triplicate.

RNA interference

The interference dsDNA sequences were cloned based on the cDNA sequence of the *Nraox* gene using antisense and sense primers (*aox*i-F and *aoxi*-R), which included the T7 promoter sequence (underlined in supplementary Table S1) at their 5-prime ends. The enhanced green fluorescent protein gene (*egfp*) was amplified from the cDNA sequence of plasmid C: Bar-eGFP with the primer pair *egfp*-F and *egfp*-R. It was used as a negative control. The dsRNA were synthesized in vitro using the MEGAscript® High Yield Transcription kit (Ambion, USA), followed by the generation of short interfering RNA (siRNA) using Short Cut RNase III (New England Biolabs) digestion, according to the manufacturer's instructions, after quantity testing using an ultraviolet spectrophotometer.

The conidial suspension was inoculated into 100 ml of SMY medium and incubated in an incubator shaking at 28 °C and 250 rpm. After 48–60 h, the blastospores were harvested by centrifugation, washed twice with cold sterile PBS and suspended in sterile deionized water to 3×10^7 blastospores/ml. The final 1.0 ml suspension was divided into 1.5 ml microtubes for transformation. The blastospore-based transformation system was modified according to the PEG/LiCl method (Moazeni et al. 2012), and siRNA, at final concentrations of 400 and 800 nM, were added to the blastospore suspensions. A positive control (wild type blastospore, without siRNA) and a negative control (wild type blastospore treated with 400 and 800 nM *egfp* siRNA) were also run with the experiment. Subsequently, the transformed blastospore suspension was used in further studies. All the experiments were performed at least three times.

Gene expression levels and intracellular H_2O_2 concentration tests after treatment with mitochondrial respiratory chain inhibitors and/or inducers of oxidative stress

CQNr01 conidiospore suspensions were inoculated in three groups of AM medium for 84 h, and then induced by 0.3 mM H_2O_2, 0.3 mM menadione and 1 mM SHAM (Sigma: dissolved in 95 % enthanol) for 1 h under the same conditions respectively. The cells were harvested and processed for RNA isolation and *Nraox* expression was assayed using real-time PCR. The above-mentioned 84 h cultures were treated by 1 mM SHAM, cultured sequentially for 5, 10, 15 and 20 min, and then harvested and subjected to intracellular H_2O_2 concentration testing using an H_2O_2 assay kit (Beyotime Biotechnology). The same experiment with ethanol substituted for the SHAM treatment was used as a control.

Growth, development and MS formation in various strains

To explore the role of *Nraox* under environmental stresses, the silenced (*Nraox*RM), positive control and negative control strains were cultured at 25 °C in which the SMAY medium was supplemented with stress effectors, such as H_2O_2 and menadione. The colony morphology was observed and images were collected using a digital camera (60-mm Macro lens, Canon Inc, Japan).

The silenced, positive control and negative control strains were cultured in AM medium. Furthermore, the CQNr01 strain was inoculated into the AM medium after being treated with the inhibitor. The mycelia and MS morphologies were observed using a microscope and digital camera. The effects of the SHAM inhibitor and gene silencing on the growth and differentiation of MS were evaluated by analyzing biomass accumulation and MS yields.

Virulence assays

To assay the virulence of various strains, aliquots of 5 µl MS suspensions in cottonseed oil (10^7 MS/ml) of the controls and RNAi-silenced strains (*Nraox*RM) were surface-inoculated into 30 third-instar larvae of *S. litura*. For the blank control, 5 µl of cottonseed oil alone was

inoculated into the larvae. The treated larvae were kept in an artificial climatic chamber at 25 ± 1 °C, 65 ± 5 % relative humidity, and a photoperiod of 16 h light: 8 h dark. All of the experiments were repeated three times. Larval mortalities were recorded everyday and the lethal time values for 50 % mortality (LT_{50}) were estimated with the infectivity of *N. rileyi*.

Statistical analysis

All experiments were performed at least three times. The quantitative data are expressed as mean ± SEM for each experiment. All statistics were analyzed by the SPSS 17.0 statistics program using a one-way analysis of variance (ANOVA) followed by Duncan's Multiple Range test. The graphs were made with the GraphPad Prism 5 program. The LT_{50} values were estimated from the trends of three repeated bioassays and by a probit analysis using SAS version 9.1 software.

Results

Gene cloning, molecular characterization and structural analysis of the *Nraox* gene

Using the available transcriptome library of CQNr01, we cloned and obtained the full-length cDNA sequence of *Nraox* (GenBank No. KM978957). A sequence analysis showed that the full-length cDNA of *Nraox* contained a 1068 bp ORF encoding a protein of 355 amino acids with a predicted molecular mass of 40.517 kDa and isoelectric point of 9.53. There is not a signal peptide in Aox (http://expasy.org/tools/protparam.html). In addition, the TargetP analysis showed that NrAox was located in the mitochondria. The genomic sequence of *Nraox* was approximately 1512 bp long and consists of three exons interrupted by two introns, corresponding to the cDNA sequence.

To examine the phylogenetic relationship of the NrAox of CQNr01 with other species, a phylogenetic tree was established using the MEGA 4.0 program. Aox proteins were highly homologous to the sequences of the entomopathogenic fungus *Metarhizium anisopliae*, belonging to the Clavicipitaceae (Fig. 1). Additionally, the homology comparison by BlastP showed that NrAox had up to 88.17 % homology with *M. anisopliae* Aox.

Nraox expression during MS development

The expression levels of the *Nraox* gene during MS development were analyzed by RT-qPCR. The results showed that *Nraox* was expressed in all developmental stages, while the highest expression level occurred in the MS initiation stage (84 h), when compared with that in the germinating spore stage (Fig. 2A).

Effects of oxidative stress and an inhibitor on the expression of *Nraox* and the generation of intracellular H_2O_2 in MS formation

We challenged MS developmental cells with different compounds that are known to generate ROS and then the corresponding *Nraox* expression levels were measured. Compared to the control, the *Nraox* expression levels were up-regulated in varying degrees when induced by both H_2O_2 and menadione. The *Nraox* expression was increased by sevenfold with an H_2O_2 treatment, whereas the transcript level was up-regulated by almost 20-fold with a menadione treatment. However, SHAM, a specific inhibitor of alternative oxidase, did not significantly impact the expression of *Nraox*. The ethanol control had no influence on *Nraox* transcript levels (Fig. 2B). At the same time, the intracellular H_2O_2 concentration after treatment with the inhibitor showed that the intracellular H_2O_2 content was higher than after the 10 min SHAM treatment but after 15 min there was no significant difference. Overall, the clean rate was a little slower than that of the wild type control (Fig. 3).

CQNr01 growth, development and MS formation after inhibitor and *Nraox*-RNAi treatments

The hyphal morphology and the MS formation of CQNr01 were examined after treatment with SHAM. Compared with the controls, the hyphal morphology after inhibitor treatment was abnormal, curved and with more bud-like structures (Fig. 4). Meanwhile, MS formation was delayed and the MS were larger and fluffier than those of the control (Fig. 5A). Additionally, the MS yields were reduced to 95 % (Table 1). The ethanol control did not impact MS formation and yields.

After treatment with 800 nM siRNA, the mRNA level in the RNAi-silenced strains declined by 76.1 % (Fig. 6). The in vitro phenotypes of the *Nraox* RNAi mutantion were analyzed on SMAY (containing 0.3 mM H_2O_2 and 0.3 mM menadione) and AM medium. A variety of morphological features were observed in the *Nraox*RM. When grown on SMAY media containing different stress inducers, there were no significant differences between wild type and *egfp*RM strains. The growth of the *Nraox*RM were slower, mycelium formation was delayed, the conidial yields were reduced (Table 2), and the colonies of *Nraox*RM were smaller (Fig. 7) compared to the wild type. In AM medium, MS was formed normally in the controls while the *Nraox*RM could not produce normal MS successfully after 3–3.5 days. In addition, the MS formed were larger than

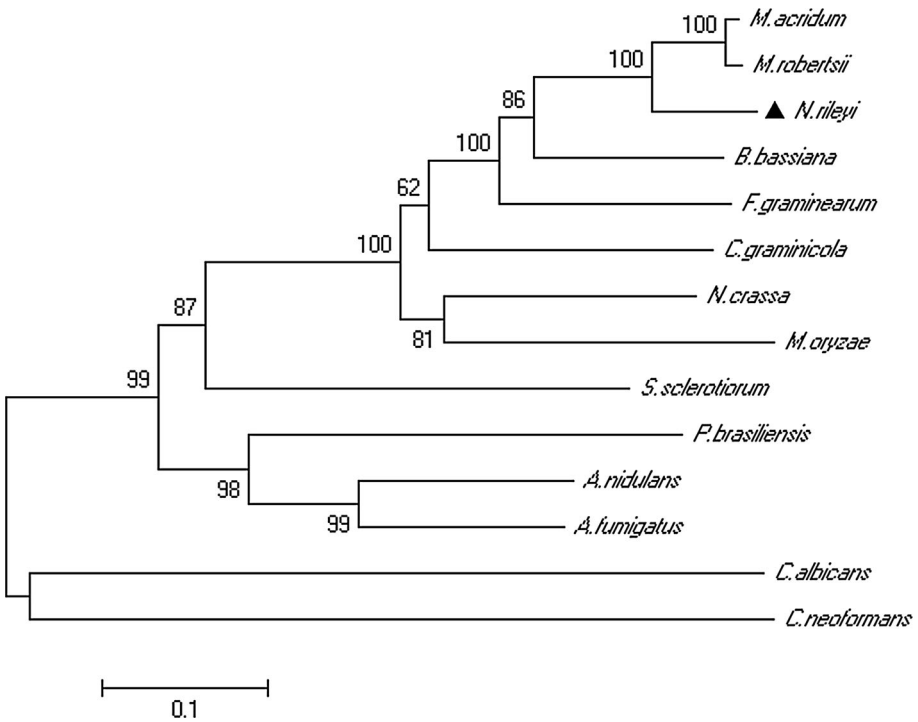

Fig. 1 Phylogenetic tree of *Nomuraea rileyi* Aox homologues constructed from different species by MEGA 4.0 (NJ) program. *Metarhizium acridum CQMa* 102 (XP_007810939.1), *Metarhizium robertsii* (EXV01183.1), *Fusarium graminearum PH-1* (ESU06647.1), *Beauveria bassiana* ARSEF 2860 (EJP63955.1), *Neurospora crassa* OR74A (XP_962086.1), *Magnaporthe oryzae* 70-15 (XP_003712663.1), *Aspergillus nidulans* (AAN39883.1), *Aspergillus fumigatus* Af29 (XP_749637.1), *Sclerotinia sclerotiorum* 1980 UF-70 (XP_001596660.1), *Colletotrichum graminicola* M1.001 (EFQ28793.1), *Paracoccidioides brasiliensis* Pb18 (EEH47663.1), *Candida albicans* (AAF21993.1), *Cryptococcus neoformans* (AAM22475.1). The numbers at each branch represent the percentage of bootstrap values in 1000 sampling replicates (Mega 4.0, Bootstraps = 1000). The *scale bar* indicates 0.1 amino acid substitutions per site

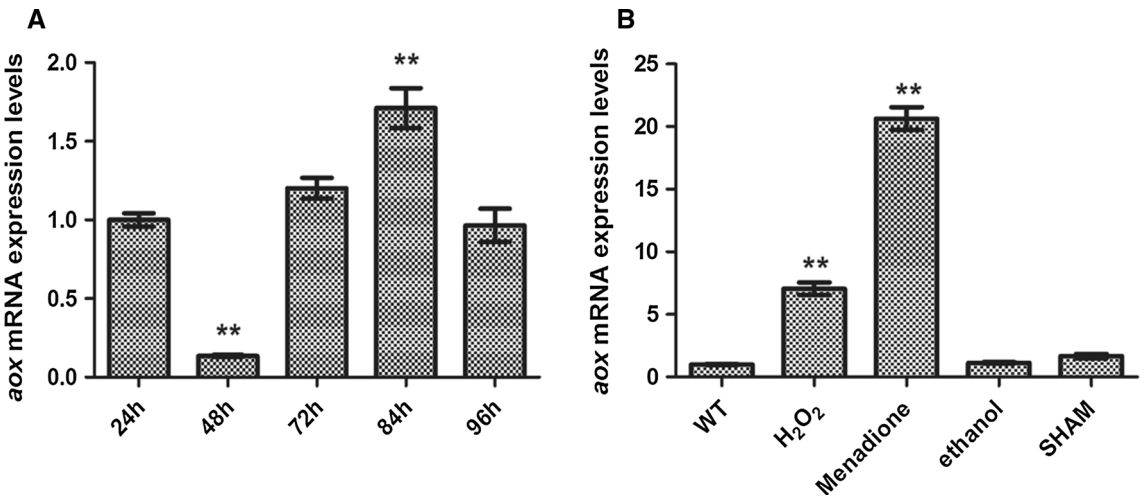

Fig. 2 The transcriptional levels of *Nraox*. **A** The transcriptional levels of *Nraox* during MS development. **B** Effects of oxidative stress on the expression levels of *Nraox* during the microsclerotia initiation stages of *Nomuraea rileyi*. The number of transcripts was determined by RT-qPCR. The results were normalized to the reference genes *tef* and *tub*. These values represent the expression levels relative to the germinating spore stage (24 h) and wild type (WT) levels, respectively. Data are presented as the mean relative expressions ±SD of results from three independent assays. The expression ratios were calculated from the cycle threshold values using the $2^{-\triangle\triangle CT}$ method, and SPSS and GraphPad Prism 5 softwares. $^{*}P < 0.05$; $^{**}P < 0.01$

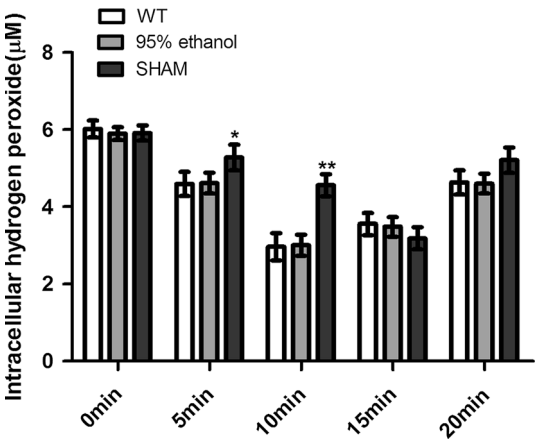

Fig. 3 Detection of intracellular H_2O_2 concentrations at different time points. Fungal cultures and compound measurements were performed as describe in the "Materials and methods". The results showed that the removal of H_2O_2 slowed after inhibitor treatments. These values are presented as the mean relative expressions ±SD of results from three independent assays. Standard *error bars* indicate variation in the measurements.*$P < 0.05$; **$P < 0.01$, when compared with the results at the same time observed in the wild type

those of the control (Fig. 5B). The abnormal hyphae in the *Nraox*RM were observed under the microscope (Fig. 4) and both MS yields and biomass were measured. The data revealed that the biomass and MS yields of *Nraox*RM were significantly reduced (Table 3), which suggested that *Nraox* was required for normal hyphal growth and MS differentiation in CQNr01.

Effects of *Nraox* on CQNr01's virulence

The pathogenicity of various strains (Table 4) was subjected to probit analysis. The mean LT_{50} (±SE) value for wild type, *egfp* and *Nraox*-RNAi strains were estimated at 8.97 ± 0.31, 9.01 ± 0.17 and 11.32 ± 0.21 days, respectively ($P < 0.05$). A knock-down of *Nraox* reduced the mortality rate of infected larvae.

Discussion

ROS plays a key role in cellular differentiation and development during pathogen invasion, which is thought to depend on MAP kinase signal transduction pathways (Scott and Eaton 2008). Mitochondria are the primary intracellular sources of ROS. An essential event during the cell growth of pathogenic fungi is the activation of mechanisms to attenuate the damage induced by ROS through the production of detoxifying molecules (Martins et al. 2011; Perrone et al. 2008). The alternative oxidase is part of the non-proton motive non-energy-conserving pathway of the mitochondrial respiratory process that lowers intramitochondrial ROS levels in fungi and plants (Maxwell et al. 1999; Van Aken et al. 2009). It has been demonstrated that inducers of oxidative stress are involved in sclerotial differentiation of filamentous phytopathogenic fungi (Papapostolou and Georgiou 2010a, b). Therefore, the NrAox of CQNr01 may have an important role in MS formation through regulating oxidative stress levels. Some studies indicate that Aox is involved in the growth pattern regulation of this fungus (Martins et al. 2011; Xu et al. 2012). Furthermore, Aox may regulate its response to oxidative stress and changes in the living environment by scavenging ROS (Magnani et al. 2007). In the present study, we have explored the involvement of NrAox during MS development and hyphal growth in *N. rileyi* CQNr01.

To study the roles *Nraox* may play in the MS formation, the full-length sequence was first isolated and analyzed. The amino acid sequence encoded by the alternative oxidase in CQNr01 is highly conserved in other species. The NrAox coding region from CQNr01 contains six conserved amino acids residues, which are proposed to be a di-iron binding motif (Siedow and Umbach 2000; Magnani et al. 2007). The *Nraox* transcriptional levels at different times during the MS formation were analyzed by RT-qPCR, and *Nraox* expression was up-regulated at the MS initiation

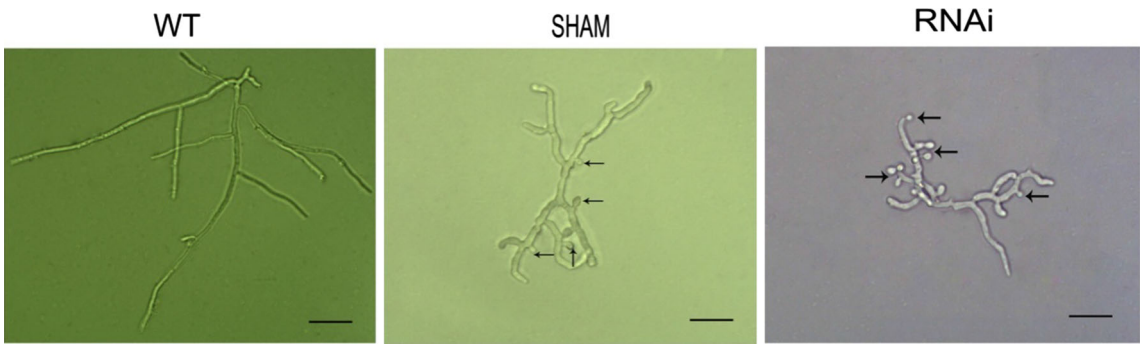

Fig. 4 Photos showing hyphal morphology after inhibitor treatments and gene silencing in *Nomuraea rileyi* grown in AM liquid medium. Hyphae were curved and more bud-like structures were formed compared with the control hyphae. *Scale bar* 100 μm

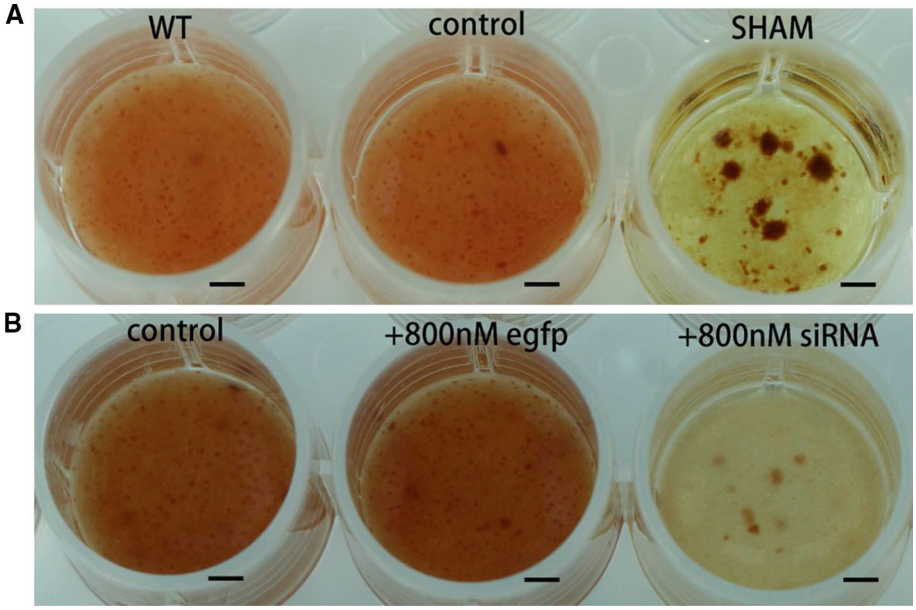

Fig. 5 The phenotype of microsclerotia in the test strains. **A** Microsclerotia phenotypes of the wild type (WT), the control and the SHAM inhibitor treated *Nomuraea rileyi* after 3 days of inoculation in AM. **B** The phenotype of MS in the control and siRNA-transformation treatments strains. Microsclerotia SHAM inhibitor-treated and *Nraox*-silenced microsclerotia were larger than those of the WT and the controls. *Scale bar* 0.5 cm

Table 1 Effect of SHAM inhibitor treatments on *Nomuraea rileyi* microsclerotia yields and biomass

SHAM (mM)	0	95 %	1
MS yields ($\times 10^4$/ml)	8.47 ± 0.11	8.61 ± 0.08	0.41 ± 0.03**
Biomass (g/l)	24.68 ± 0.32	24.97 ± 0.28	7.2 ± 0.47**

* $P < 0.05$, ** $P < 0.01$, when compared with the results observed at wild type

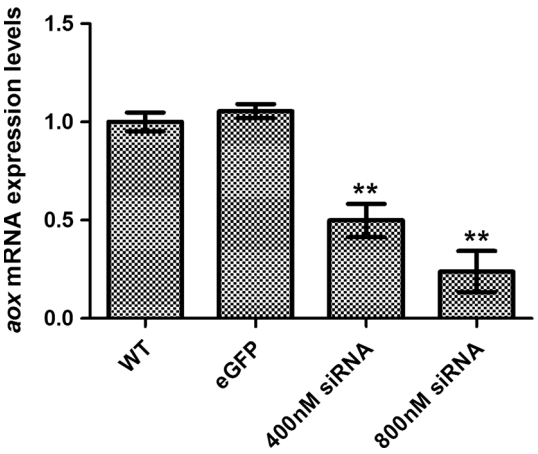

Fig. 6 Effects of siRNA interference on *Nraox* transcript levels. The *Nraox* transcripts number was normalized as previously described. Transformation with *egfp*-siRNA was the negative control. The *Nraox* expression level values are averages of standard errors of the means (SEMs) of the results from three independent assays. *$P < 0.05$; **$P < 0.01$

Table 2 Conidial yields analysis of different strains grown under two stress effector treatments

Strains	Conidial yields ±SE ($\times 10^8$ conidia/cm^2)	
	0.3 mM H_2O_2	0.3 mM menadione
WT	6.52 ± 0.24	6.39 ± 0.28
*egfg*RM	6.49 ± 0.25	6.31 ± 0.31
*Nraox*RM	3.08 ± 0.33**	1.31 ± 0.43**

* $P < 0.05$, ** $P < 0.01$, when compared with the results observed at wild type

stage, indicating that *Nraox* plays a critical role in MS formation.

Aox has been reported to be up-regulated in fungi under mitochondrial respiratory chain inhibition and/or oxidative stress conditions (Huh and Kang 2001; Johnson et al. 2003; Joseph-Horne et al. 2001; Magnani et al. 2007; Martins et al. 2011), which is in agreement with our results that *Nraox* expression was induced by ROS-generating compounds. Thus the *aox* up-regulated expression is closely related to intracellular oxidative stress. SHAM had no effect on *Nraox* expression, which was consistent with the results from Martins et al. (2011). Those results suggest that Aox activity does not control its own expression. However, after SHAM treatment, the removal of intracellular H_2O_2 was significantly blocked. These results corroborate a report for *Capsicum annuum* inhibition of alternative oxidase (Purvis 1997). Therefore, ROS may be common messengers for the induction of *aox* expression and *aox* is involved in the resistance to oxidative stress in fungi. Under normal culture conditions, the inhibition of Aox by SHAM changed hyphal morphology, decreased MS

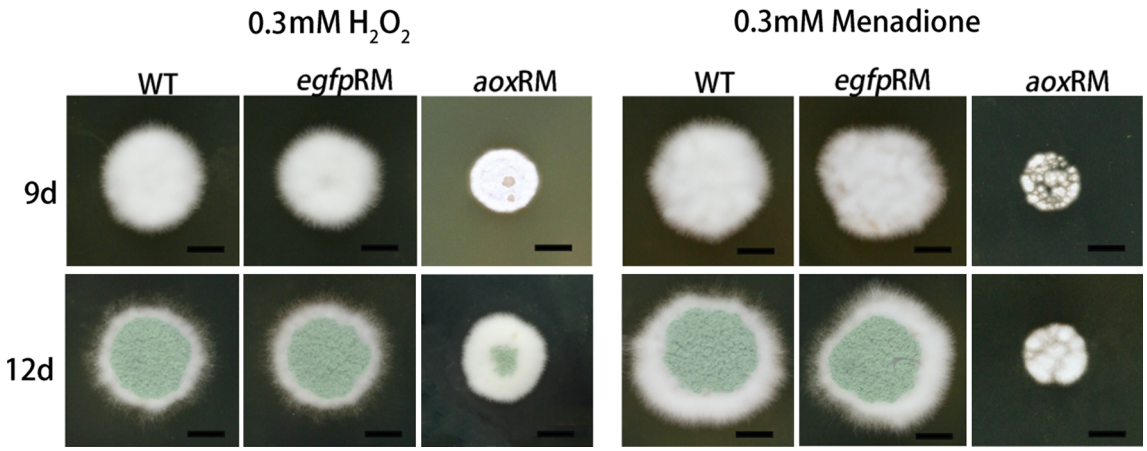

Fig. 7 Colony morphology of control and *Nraox*-silenced strains. Strains were grown in the presence of stress effectors (H_2O_2 and menadione) in SMAY medium for 9 and 12 days. Colony growth was slower and the mycelial biomass decreased in the RNAi-silenced strains when compared with those in the controls. *Scale bar* 0.5 cm

Table 3 Analysis of microsclerotia yields and biomass of different strains grown on liquid AM

Strains	Microsclerotia yields ($\times 10^4$/ml)	Biomass (g/l)
WT	7.3 ± 0.13	21.52 ± 0.38
*egfp*RM	7.28 ± 0.10	20.94 ± 0.31
*Nraox*RM	0.20 ± 0.02**	3.07 ± 0.35**

* $P < 0.05$, ** $P < 0.01$, when compared with the results observed at wild type

yields and delayed formation of MS in the medium, indicating that *Nraox* expression was important during mycelial growth and MS formation. This finding is similar with the findings on the hyphal morphology and MS formation in other fungi, including *Ustilago maydis* (Juarez et al. 2006) and *Sclerotinia sclerotiorum* (Xu et al. 2012).

Aox may play important roles during the resistance or adaption of higher plants against abiotic stresses (Rachmilevitch et al. 2007; Ribas-Carbo et al. 2000), and RNAi technology was selected to study the gene function of *Nraox*, because other deletion technologies were not available in our laboratory. After silencing the *Nraox* gene, the mutant strain was sensitive to abiotic stresses, and growth rate and conidial yield decreased (Fig. 7). Furthermore, *Nraox* silencing caused changes in hyphal morphology (Fig. 4) and MS size (Fig. 5B). In addition, MS development was badly limited (Table 2). These findings were similar to the results of SHAM treatments, demonstrating that *Nraox* may be involved in hyphal growth and MS formation. The intracellular H_2O_2 concentration was not significantly different between the strains (data no shown). The reason may be that another enzyme supplies the alternative oxidase scavenging H_2O_2.

MS served as a hyphal aggregate, reproductive structure and exhibited insecticidal activity (Jackson and Jaronski 2009; Song et al. 2014). In the present study, MS exhibited insecticidal efficacy against *S. litura*, and the silencing of *Nraox* weakened the virulence of *N. rileyi* significantly. The MS from *Nraox*RM significantly decreased the virulence. The LT_{50} value of MS from *Nraox*RM increased by 26.2 % after being inoculated into *S. litura*. Likewise, the toxicity of the *Cryptococcus neoformans aox1* mutant strain was greatly reduced, which suggests that Aox contributes to the virulence of this organism (Akhter et al. 2003). In *Paracoccidioides brasiliensis*, PbAOX was proven to be relevant to virulence (Ruiz et al. 2011). However, in *Magnaporthe grisea*, the *aox* gene mutant strain's pathogenicity was retained without a significant impairment in virulence (Avila-Adame and Koller 2003). Thus, the *Nraox* functions related to the pathogenicity need to further study.

In the present study, the *Nraox* gene was cloned from *N. rileyi*. The expression profile analysis and *Nraox* silencing demonstrated that *Nraox* plays an important role in MS differentiation by regulating the intracellular redox balance and hypha growth. Furthermore, *Nraox* was found to be essential for virulence in CQNr01. Studies are

Table 4 Mortality percentage and probit model parameters (LT_{50}) of various strains

	Mortality (% ± SE)	LT_{50} (days ± SE)	95 % confidence interval (days)
Control	96.31 ± 0.84	8.97 ± 0.31	8.12–9.7
*egfp*RM	95.82 ± 1.13	9.01 ± 0.17	8.59–9.43
*Nraox*RM	89.05 ± 1.21**	11.32 ± 0.21**	10.80–11.84

* $P < 0.05$, ** $P < 0.01$, when compared with the results observed at control

currently underway to provide insights into both the molecular mechanism of MS differentiation and the control of insects by MS in *N. rileyi*.

Acknowledgments This work was supported by the Special Fund for Agro-Scientific Research in the Public Interest (Project No. 201103002) and the State High Technique Program (863) of China (Project No. 2011AA10A201).

References

Akhter S, McDade HC, Gorlach JM et al (2003) Role of alternative oxidase gene in pathogenesis of *Cryptococcus neoformans*. Infect Immun 71(10):5794–5802

Avila-Adame C, Koller W (2003) Impact of alternative respiration and target-site mutations on responses of germinating conidia of *Magnaporthe grisea* to Qo-inhibiting fungicides. Pest Manag Sci 59(3):303–309

Faria MRd, Wraight SP (2007) Mycoinsecticides and mycoacaricides: a comprehensive list with worldwide coverage and international classification of formulation types. Biol Control 43(3):237–256

Georgiou DC (1997) Lipid peroxidation in *Sclerotium rolfsii*: a new look into the mechanism of sclerotial biogenesis in fungi. Mycol Res 101(4):460–464

Georgiou DC, Tairis N, Sotiropoulou A (2000a) Hydroxyl radical scavengers inhibit lateral-type sclerotial differentiation and growth in phytopathogenic fungi. Mycologia 92(5):825–834

Georgiou DC, Tairis N, Sotiropoulou A (2000b) Hydroxyl radical scavengers inhibit sclerotial differentiation and growth in *Sclerotinia sclerotiorum* and *Rhizoctonia solani*. Mycol Res 104:1191–1196

Georgiou DC, Patsoukis N, Papapostolou L et al (2006) Sclerotial metamorphosis in filamentous fungi is induced by oxidative stress. Integr Comp Biol 46(6):691–712

Goldman GH, dos Reis Marques E, Duarte Ribeiro DC et al (2003) Expressed sequence tag analysis of the human pathogen *Paracoccidioides brasiliensis* yeast phase: identification of putative homologues of *Candida albicans* virulence and pathogenicity genes. Eukaryot Cell 2(1):34–48

Harman D (1956) Aging: a theory based on free radical and radiation chemistry. J Gerontol 11(3):298–300

Harman D (1981) The aging process. Proc Natl Acad Sci USA 78(11):7124–7128

Harman D (1998) Aging and oxidative stress. J Int Fed Clin Chem 10(1):24–27

Hattori T, Honda Y, Kino K et al (2008) Expression of alternative oxidase gene (*aox1*) at the stage of single-cell conidium in citric acid-producing *Aspergillus niger*. J Biosci Bioeng 105(1):55–57

Helmerhorst EJ, Stan M, Murphy MP et al (2005) The concomitant expression and availability of conventional and alternative, cyanide-insensitive, respiratory pathways in *Candida albicans*. Mitochondrion 5(3):200–211

Huh WK, Kang SO (2001) Characterization of the gene family encoding alternative oxidase from *Candida albicans*. Biochem J 356(2):595–604

Jackson MA, Jaronski ST (2009) Production of microsclerotia of the fungal entomopathogen *Metarhizium anisopliae* and their potential for use as a biocontrol agent for soil-inhabiting. Mycol Res 113(8):842–850

Jiang SS, Yin YP, Song ZY et al (2014) RacA and Cdc42 regulate polarized growth and microsclerotium formation in the dimorphic fungus *Nomuraea rileyi*. Res Microbiol 165(3):233–242

Johnson CH, Prigge JT, Warren AD et al (2003) Characterization of an alternative oxidase activity of *Histoplasma capsulatum*. Yeast 20(5):381–388

Joseph-Horne T, Hollomon DW, Wood PM (2001) Fungal respiration: a fusion of standard and alternative components. Biochim Biophys Acta 1504(2–3):179–195

Juarez O, Guerra G, Velazquez I et al (2006) The physiologic role of alternative oxidase in *Ustilago maydis*. FEBS J 273(20):4603–4615

Liu JJ, Yin YP, Song ZY et al (2014) NADH: flavin oxidoreductase/NADH oxidase and ROS regulate microsclerotium development in *Nomuraea rileyi*. World J Microbiol Biotechnol 30(7):1927–1936

Livak KJ, Schmittgen TD (2001) Analysis of relative gene expression data using real-time quantitative PCR and the $2^{-\Delta\Delta Ct}$ method. Methods 25(4):402–408

Magnani T, Soriani FM, Martins VP et al (2007) Cloning and functional expression of the mitochondrial alternative oxidase of *Aspergillus fumigatus* and its induction by oxidative stress. FEMS Microbiol Lett 271(2):230–238

Martins VP, Dinamarco TM, Soriani FM et al (2011) Involvement of an alternative oxidase in oxidative stress and mycelium-to-yeast differentiation in *Paracoccidioides brasiliensis*. Eukaryot Cell 10(2):237–248

Maxwell DP, Wang Y, McIntosh L (1999) The alternative oxidase lowers mitochondrial reactive oxygen production in plant cells. Proc Natl Acad Sci USA 96(14):8271–8276

McDonald AE (2008) Alternative oxidase: an inter-kingdom perspective on the function and regulation of this broadly distributed cyanide-resistant terminal oxidase. Funct Plant Biol 35(7):535–552

Moazeni M, Khoramizadeh MR, Kordbacheh P et al (2012) RNA-mediated gene silencing in *Candida albicans*: inhibition of hyphae formation by use of RNAi technology. Mycopathologia 174(3):177–185

Papapostolou I, Georgiou CD (2010a) Hydrogen peroxide is involved in the sclerotial differentiation of filamentous phytopathogenic fungi. J Appl Microbiol 109(6):1929–1936

Papapostolou I, Georgiou CD (2010b) Superoxide radical is involved in the sclerotial differentiation of filamentous phytopathogenic fungi: identification of a fungal xanthine oxidase. Fungal Biol 114(5–6):387–395

Perrone GG, Tan SX, Dawes IW (2008) Reactive oxygen species and yeast apoptosis. Biochim Biophys Acta 1783(7):1354–1368

Purvis AC (1997) Role of the alternative oxidase in limiting superoxide production by plant mitochondria. Physiol Plant 100:165–170

Rachmilevitch S, Xu Y, Gonzalez-Meler MA et al (2007) Cytochrome and alternative pathway activity in roots of thermal and non-thermal Agrostis species in response to high soil temperature. Physiol Plant 129:163–174

Ribas-Carbo M, Aroca R, Gonzalez-Meler MA et al (2000) The electron partitioning between the cytochrome and alternative respiratory pathways during chilling recovery in two cultivars of maize differing in chilling sensitivity. Plant Physiol 122(1):199–204

Ruiz HO, Gonzalez A, Almeida AJ et al (2011) Alternative oxidase mediates pathogen resistance in *Paracoccidioides brasiliensis* infection. PLoS Negl Trop Dis 5(10):e1353

Ruy F, Vercesi AE, Kowaltowski AJ (2006) Inhibition of specific electron transport pathways leads to oxidative stress and decreased Candida albicans proliferation. J Bioenerg Biomembr 38(2):129–135

Schonbaum GR, Bonner WD Jr, Storey BT et al (1971) Specific inhibition of the cyanide-insensitive respiratory pathway in plant mitochondria by hydroxamic acids. Plant Physiol 47(1):124–128

Scott B, Eaton CJ (2008) Role of reactive oxygen species in fungal cellular differentiations. Curr Opin Microbiol 11(6):488–493

Siedow JN, Umbach AL (2000) The mitochondrial cyanide-resistant oxidase: structural conservation amid regulatory diversity. Biochim Biophys Acta 1459(2–3):432–439

Song ZY, Yin YP, Jiang SS et al (2013) Comparative transcriptome analysis of microsclerotia development in *Nomuraea rileyi*. BMC Genom 14:411

Song ZY, Yin YP, Jiang SS et al (2014) Optimization of culture medium for microsclerotia production by *Nomuraea rileyi* and analysis of their viability for use as a mycoinsecticide. Biocontrol 59:597–605

Suwannakut S, Boucias DG, Wiwat C (2005) Genotypic analysis of *Nomuraea rileyi* collected from various noctuid hosts. J Invertebr Pathol 90(3):169–176

Thakre M, Thakur M, Malik N et al (2011) Mass scale cultivation of entomopathogenic fungus *Nomuraea rileyi* using agricultural products and agro wastes. J Biopestic 4(2):176–179

Van Aken O, Giraud E, Clifton R et al (2009) Alternative oxidase: a target and regulator of stress responses. Physiol Plant 137(4):354–361

Vanlerberghe GC, Mclntosh L (1997) Alternative oxidase: from gene to function. Annu Rev Plant Physiol Plant Mol Biol 48:703–734

Xu T, Yao F, Liang WS et al (2012) Involvement of alternative oxidase in the regulation of growth, development, and resistance to oxidative stress of *Sclerotinia sclerotiorum*. J Microbiol 50(4):594–602

Yin YP, Huang S, Song ZY et al (2012) Microsclerotia artificial inductions of *Nomuraea rileyi* CQNr01. Sci Agric Sin 45(23):4801–4807 **(In Chinese)**